Geophysical Journal International

Geophys. J. Int. (2021) **226,** 610–616
Advance Access publication 2021 March 25
GJI Gravity, Geodesy and Tides

doi: 10.1093/gji/ggab113

Polar motion resonance in the prograde diurnal band

I. Nurul Huda,[1,2] C. Bizouard,[2] D. Allain[3] and S. Lambert[2]

[1]*Department of Astronomy and Bosscha Observatory, Institut Teknologi Bandung, Bandung,* 40116*, Indonesia. E-mail: ibnu.nurulhuda@obspm.fr*
[2]*Observatoire de Paris/SYRTE, Université PSL, CNRS, Sorbonne Université, Paris,* 75014*, France*
[3]*Observatoire Midi-Pyrénées/LEGOS, Toulouse,* 31400*, France*

Accepted 2021 0. Received 2021 February 16; in original form 2020 October 6

SUMMARY

Until now, the polar motion resonance (PMR) complex frequency has been determined in the seasonal and retrograde diurnal band of the polar motion. In this study, this resonance is studied in the prograde diurnal band, where polar motion is mainly composed of periodic terms caused by the diurnal oceanic tide. The resonance parameters (period and quality factor) are encompassed in the frequency transfer function between generating tidal potential and polar motion, and can be estimated accordingly. To this aim, we gather three published sets of prograde diurnal terms determined from Global Navigation Satellite System (GNSS) and Very Long Baseline Interferometry (VLBI), to which we append our own estimates based upon a processing of the VLBI delays over the period 1990–2020. Then, by fitting the PMR parameters so that the prograde diurnal terms match the corresponding components of the tide generating potential, we obtained a resonance period of about 401 d and an equivalent quality factor of −22, differing from those reigning in the seasonal band ($P_{\rm PMR} \approx 431$ d; $Q_{\rm PMR} \approx$ 56–255) and in the retrograde diurnal band ($P_{\rm PMR} \approx 380$ d; $Q_{\rm PMR} \approx -10$). Our estimates confirm strikingly the theoretical prediction derived from the tidal ocean angular momentum derived from the FES 2014 ocean tide model.

Key words: Earth rotation variations; Geodetic instrumentation; Rheology: mantle.

1 INTRODUCTION

As soon as the displacement of the Earth's rotation pole with respect to the Earth crust—the polar motion—has been discovered, it arouses a great interest for studying the Earth rheology. First, its main component, named *Chandler wobble*, is a normal mode, of which the period is fixed by the Earth properties. Such a mode had been foreseen by L. Euler in the middle of the 18th century as a consequence of the Earth dynamical flattening e, namely the relative difference between axial and equatorial moments of inertia of the Earth, $(C - A)/A = 3.2845479(1) \times 10^{-3}$ (Mathews *et al.* 2002): the rotation axis $I_{\rm R}$ freely rotates around the main inertia axis $I_{\rm C}$ in the body frame at the *Euler angular frequency* $\sigma_{\rm e} = (C - A)/A\Omega$, where $\Omega = 7.2921150 \times 10^{-5}$ rad s^{-1} is the Earth's angular velocity of reference. However, with a period of about 304 d, the Euler prediction was seemingly in contradiction with the 430-d period detected by Chandler in 1891 from latitude observations.

This issue was solved in the following years, in particular by Newcomb, who advocated the Earth's non-rigidity as the factor lengthening the Euler period from 304 to 430 d. His argumentation is the following. As the rotation axis moves with respect to the terrestrial reference system, the centrifugal force varies accordingly. This variation can be represented by the gradient of a tesseral potential depending on pole displacement and called *pole tide* potential by analogy to the lunisolar potential. The non-rigid Earth tends to readjust its equatorial bulge around the instantaneous rotation axis, and the whole Earth undergoes a variable deformation, accompanying the pole displacement. The less rigid is the Earth, the larger is this *pole tide deformation*. In the body reference system Gxyz, aligned with the mean principal axes ($Gx = I_{\bar{\rm A}}$, $Gz = I_{\bar{\rm C}}$), the instantaneous main inertia axis $I_{\rm C}$ will shift towards the instantaneous rotation axis $I_{\rm R}$, so that the instantaneous moment of inertia around $Gz = I_{\bar{\rm C}}$ decreases accordingly; so seen from the terrestrial system we have an apparent compensation of the dynamical ellipticity, the apparent Euler frequency decreases and the corresponding period increases up to the observed value of 433 ± 1 d (according to contemporaneous observations). As the pole tide deformation is accompanied by dissipation, the Chandler wobble is damped, with a quality factor in the interval (56, 255) (Nastula & Gross 2015).

In the common band of the polar motion, stretching from some days to subsecular timescale, it is commonly assumed that the Earth rheology is the same. An Earth composed of a quasi-elastic mantle, a passive core and hydrostatic oceans allows to account for the aforementioned resonance parameters. However, below 10 d, the ocean behaves dynamically, and the ocean pole tide is modified accordingly. This issue was addressed recently by Bizouard *et al.* (2020) for the retrograde diurnal band of the polar motion, equivalently the nutation band in the celestial system, where the polar motion resonance (PMR) appears at the period of about 380 d with

respect to the terrestrial reference system and apparent damping coefficient becomes negative according to nutation analysis. In light of an ocean tide model, the authors showed that this striking change of the resonance parameters is caused by the dynamical response of the oceans. Besides, they present some observational evidence that the resonance period is also affected by the free core nutation resonance in the retrograde diurnal band.

In order to get a more comprehensive picture, this kind of analysis has to be extended to other frequency bands. In this paper, we investigate the Earth response in the prograde diurnal band of the polar motion, which had not been done until now to our knowledge. In contrast to the retrograde diurnal band, the prograde polar motion of the Celestial Intermediate Pole is mainly caused by the ocean tides, but the generating potential is still tesseral.

After having reminded the lineaments of the polar motion theory and how polar motion is forced by ocean and body tides (Section 2), we derive a theoretical prediction of PMR parameters from the FES 2014 ocean tide model (Section 3). In Section 4, we expose our own estimation of the prograde diurnal terms through VLBI observation processing. Then, in Section 5, our estimates of the prograde diurnal terms as well as published estimates are used along with the corresponding components of the lunisolar tidal potential to determine the PMR parameters, and to test the theoretical prediction done in Section 3.

2 POLAR MOTION RESONANCE PARAMETERS

The PMR parameters depend on the Earth response to the tesseral rotational potential generated by the polar motion itself in the terrestrial system, and therefore are determined by the Earth rheology. For a tesseral potential of degree 2 and order 1, it reads (Dehant & Mathews 2015)

$$W_2 = -\frac{\Omega^2 R_e^2}{3} \Re\left[\tilde{\Phi}(t) Y_2^{-1}(\theta,\lambda)\right], \tag{1}$$

with

$$\tilde{\Phi}(t) = \frac{3gN_2^1}{\Omega^2 R_e^2} \sum_{\sigma\geq 0} \xi_\sigma e^{i(\theta_\sigma(t)-\pi/2)}, \tag{2}$$

where R_e is the mean equatorial radius, $Y_2^{-1} = P_2^1(\cos\theta)e^{-i\lambda}$ (with θ the colatitude and λ the longitude), g is the mean Earth equatorial gravity, ξ_σ is the equilibrium tidal height, $(N_2^1)^2 = 5/24\pi$ and θ_σ is the tidal argument of the corresponding frequency.

For the solid Earth, the degree 2 Stokes coefficients C_{21} and S_{21} of the geopotential undergo variations ΔC_{21} and ΔS_{21} such that

$$\frac{GM}{R_e} \Re\left[(\Delta C_{21} + i\Delta S_{21}) Y_2^{-1}\right] = k_2 W_2, \tag{3}$$

where k_2 is the Love number relevant to the frequency band. By putting expression (1) of W_2 in (3), we obtain

$$\Delta C_{21} + i\Delta S_{21} = -k_2 \frac{\Omega^2 R_e^3}{3GM} \tilde{\Phi}(t). \tag{4}$$

Equivalently, in the terrestrial reference system, the off-diagonal Earth moments of inertia $I_{13} = -MR_e^2 C_{21}$ and $I_{23} = -MR_e^2 S_{21}$ vary by

$$\Delta I_{13} + i\Delta I_{23} = k_2 \frac{\Omega^2 R_e^5}{3G} \tilde{\Phi}(t) = \frac{k_2}{k_s}(C-A)\tilde{\Phi}(t), \tag{5}$$

where $k_s = 3G(C-A)/(\Omega^2 R_e^5) \approx 0.938$ is the secular Love number. At timescales of the common polar motion stretching from some days to some years, the quasi-elastic regime applies, yielding $\tilde{k}_2 = 0.307 - i0.0035$. The tilde indicates that the quantity contains an imaginary part, here associated with dissipation.

The response of the oceans is formulated in an analogue way through the ocean Love number $\tilde{k}_o$. For periods much larger than 1 day, the ocean masses redistribute hydrostatically, leading to $\tilde{k}_o \sim 0.047$. However, below 10 d the behaviour of the ocean becomes dynamical, and in turn $\tilde{k}_o$ is strongly modified. The estimation of $\tilde{k}_o$ in the diurnal band can be performed for specific tidal lines in light of an ocean tide model. Such an approach had been initiated for the retrograde diurnal band in Bizouard *et al.* (2020).

Combining the ocean and solid Earth responses to the tesseral potential, we have the rotational excitation function

$$\chi^r = \frac{\Delta I_{13} + i\Delta I_{23}}{C-A} = \frac{\tilde{k}}{k_s}\tilde{\Phi}(t), \tag{6}$$

where $\tilde{k} = \tilde{k}_2 + \tilde{k}_o$. Actually, at diurnal and subdiurnal timescales, the ocean response is dynamical, and current are generated by the tidal potential. In turn, to the mass term (6) we have to append an equatorial relative angular momentum h. Therefore, a full characterization of the rotational response is given through the rotational excitation

$$\chi^r = \frac{\Delta I_{13} + i\Delta I_{23}}{(C-A)} + \frac{h}{(C-A)\Omega} = \frac{\tilde{k}}{k_s}\tilde{\Phi}(t), \tag{7}$$

where $\tilde{k}$ now accounts for the dynamical oceanic response.

From the expression (1) it is clear that W_2 has exactly the same form than the pole tide potential $\Delta U^{(r)} = \frac{-\Omega^2 R_e^2}{3} \Re\left[m(t) Y_2^{-1}(\theta,\lambda)\right]$. Hence, the coefficient $\tilde{\Phi}(t)$ is formally equivalent to the instantaneous rotation pole $m(t)$ in pole tide potential. Let $p = x - iy$ be the complex pole coordinate of the Celestial Intermediate Pole, as observed through astrogeodetic techniques, and linked to m by the relation $m = p - i\dot{p}/\Omega$, let χ^{eff} be the effective angular momentum function accounted for mass redistribution. Accounting for pole tide by putting $\tilde{\Phi}(t) = m(t)$ in eq. (7), and accounting for the fluid core in Liouville equations leads to

$$p + \frac{i}{\tilde{\sigma}_{\text{PMR}}}\dot{p} = \chi^{\text{eff}}. \tag{8}$$

with

$$\tilde{\sigma}_{\text{PMR}} = e\Omega \frac{A}{A_m}\left(1 - \frac{\tilde{k}_2 + \tilde{k}_o}{k_s}\right), \tag{9}$$

where A_m is the mean equatorial moment of inertia of the mantle.

Here, $\tilde{\sigma}_{\text{PMR}} = 2\pi/P_{\text{PMR}}(1 + i/2Q_{\text{PMR}})$ is the complex angular frequency of the PMR, encompassing the resonance parameters, namely the period P_{PMR} and the quality factor Q_{PMR}. The $\tilde{\sigma}_{\text{PMR}}$ has to be distinguished from the observed Chandler wobble resonance. Indeed, as a resonant process, the Chandler wobble does not result from a single harmonic excitation at the resonance frequency, but from a broad-band process surrounding the resonance frequency. If the spectral content of the excitation dominates at a slightly different frequency, this one will determine the observed Chandler wobble frequency. In contrast, the PMR frequency $\tilde{\sigma}_{\text{PMR}}$ is fixed by the properties of the Earth and does not depend on the forcing. The PMR frequency is the resonance frequency describing the response (the polar motion) to excitations with a frequency that may be far from the Chandler wobble frequency. In the frequency band of the common polar motion, stretching from a few days to some years, the PMR parameters can be confused with the period and quality factor of the Chandler wobble. However, for other timescales, such a confusion is no more possible, for the global rheological parameters

determining $\tilde{\sigma}_{\rm PMR}$, namely $\tilde{k}_2$ and $\tilde{k}_{\rm o}$, deviate significantly from their values prevailing in the Chandler frequency band. So, as a rule of thumbs, the PMR complex frequency differs from the complex frequency of the Chandler wobble (see e.g. Mathews *et al.* 2002; Bizouard 2020).

Several authors have estimated the PMR parameters for the common polar motion, and found a period of about 430–433 d with the quality factor in the range of [34, 255] (see e.g. Furuya & Chao 1996; Kuehne *et al.* 1996; Nastula & Gross 2015; Vondrák *et al.* 2017). Meanwhile, from nutation analysis, many studies (see e.g. Mathews *et al.* 2002; Rosat *et al.* 2016; Nurul Huda *et al.* 2020; Ziegler *et al.* 2020) evidenced that, in the retrograde diurnal band, the PMR has a period shorter than in the seasonal band (∼380 d) and that the complex part becomes negative (corresponding to an *equivalent* quality factor of −10). As shown in Bizouard *et al.* (2020), the shortening of the PMR in the retrograde diurnal band is mainly caused by the dynamical response of the oceans to the pole tide potential, and the associated negative quality factor reflects the strong phase-shift of this response with respect to the pole tide.

3 THEORETICAL PREDICTION OF THE POLAR MOTION RESONANCE IN THE PROGRADE DIURNAL BAND

As for the retrograde diurnal band, the oceanic Love number can be determined from the knowledge of an ocean tidal model, and its subsequent effect on the ocean angular momentum. In this study we adopted one of the most recent models, namely the FES 2014 hydrodynamic model (Carrere *et al.* 2015) and considered the five main diurnal constituents $J1, K1, P1, O1$ and $Q1$. The corresponding amplitude and phase of the equatorial ocean angular momentum, as calculated from the model outputs by one of us (D. Allain), are provided in Table 1. From those quantities the prograde matter term H^+ and motion term h^+ are derived according to

$$H^+ = \frac{H_1\cos\Phi_1 + H_2\sin\Phi_2}{2} + i\,\frac{-H_1\sin\Phi_1 + H_2\cos\Phi_2}{2},$$
$$h^+ = \frac{h_1\cos\phi_1 + h_2\sin\phi_2}{2} + i\,\frac{-h_1\sin\phi_1 + h_2\cos\phi_2}{2}, \qquad (10)$$

where the coefficients H_1, H_2, Φ_1 and Φ_2 correspond to the matter term whereas the coefficients h_1, h_2, ϕ_1 and ϕ_2 correspond to the motion term of the ocean angular momentum.

The matter term is related to the moments of inertia change of the ocean $H^+ = \Omega(\Delta I_{13} + i\Delta I_{23})$. Accounting for the deformation produced by the ocean loading the effective matter term is $(1 + k'_2)H^+$ where $k'_2 = -0.3075$ is the loading Love number.

The oceanic Love number $\tilde{k}_{\rm o}$ can be derived accordingly for the five tidal components. From (7) limited to the ocean response, the $\tilde{k}_{\rm o}$ in prograde diurnal band is given by

$$\tilde{k}_{\rm o}(\sigma) = k_{\rm s}\frac{H^+(\sigma)(1+k'_2) + h^+(\sigma)}{(C-A)\Omega\tilde{\Phi}(\sigma)}. \qquad (11)$$

As shown in the last column of Table 1, the amplitude of the oceanic love number $\tilde{k}_{\rm o}$ in the prograde diurnal band is smaller compared to the oceanic Love number value $k_{\rm o} = 0.047$ in the seasonal band. The imaginary part of $\tilde{k}_{\rm o}$ is related to the delay of the ocean tide to the lunisolar force. The small frequency dependence of the values of $\tilde{k}_{\rm o}$ in Table 1 can be described by a degree two polynomial of the frequency f in cpd as follows:

$$\tilde{k}_{\rm o}(f) = (-0.5575 + i0.8714)f^2 + (1.0866 - i1.7092)f + (-0.5207 + i0.8505). \qquad (12)$$

Then, the theoretical value of PMR in the prograde diurnal band is derived by taking in eq. (9) the $\tilde{k}_{\rm o}$ expression (12). We obtain the theoretical prediction of PMR parameters displayed in Fig. 1. It turns out that, in the band [+0.89, +1.04] cpd (corresponding to the available tidal lines), the PMR period sweeps the interval [398.1, 400.3] days (with an average value of 399.5, dispersion of 0.8 d), whereas the equivalent quality factor lies in the interval [−29, −18].

On the other hand, these PMR values can be estimated by confronting the observed polar motion in the prograde diurnal, which results mostly from oceanic tides, to the lunisolar potential, according to the polar motion theory that has been sketched in Section 2.

4 ESTIMATION OF PROGRADE DIURNAL TERMS FROM VLBI

The subdiurnal tidal variations in polar motion have been determined since the beginning of the 1990s from VLBI observation (see e.g. Sovers *et al.* 1993; Herring & Dong 1994; Gipson 1996) and from SLR (see e.g. Watkins & Eanes 1994). More recently, from the processing of 20 yr of GNSS observations, Sibois *et al.* (2017) determined pole coordinates at 15 min time resolution and fitted complex semi-diurnal and diurnal amplitudes to the obtained time-series. For VLBI, estimations of tidal terms were carried out by using different approaches. Some studies have estimated the tidal terms directly from VLBI time delays (see e.g. Sovers *et al.* 1993; Herring & Dong 1994; Gipson 1996) while other (Böhm *et al.* 2012) estimated the terms indirectly from VLBI Earth orientation parameters time-series with a subdaily resolution. An intermediate approach was considered by Artz *et al.* (2011) who first determined session-wise Earth orientation parameters and then transformed them to tidal terms at the level of normal equations. The direct approach is the most precise one since it allows a rigorous propagation of the delay errors into the estimated parameters and the use of all available covariance information. We adopted this approach.

The tidally driven polar motion can be represented by the sum of circular uniform motions as follows:

$$\Delta x - i\,\Delta y = \sum_j \left(A_j^+ \mathrm{e}^{i\,\theta_j(t)} + A_j^- \mathrm{e}^{-i\,\theta_j(t)}\right), \qquad (13)$$

where $A^+ = A^+_{({\rm IP};j)} + i\,A^+_{({\rm OP};j)}$ and $A^- = A^-_{({\rm IP};j)} + i\,A^-_{({\rm OP};j)}$ are the complex amplitudes of the prograde and retrograde terms, respectively. The IERS conventions (Petit & Luzum 2010) recommend the subdiurnal polar motion series from a modified version of Ray *et al.* (1994) which is based on the global numerical ocean tide model. Our corrections are fit with respect to this model, hereafter called IERS model. So the complex amplitudes A_j^+ are decomposed into

$$A_j^+ = A^+_{({\rm IERS};j)} + \Delta A_j^+, \qquad (14)$$

where $A^+_{({\rm IERS};j)} = A^+_{({\rm OT};j)} + A^+_{({\rm LIB};j)}$ are the complex amplitudes of the IERS convention model; they can be separated into the ocean tidal terms $A^+_{({\rm OT};j)}$ and the libration terms $A^+_{({\rm LIB};j)}$. Here ΔA_j^+ are the offsets that are estimated from the VLBI observation. The *a priori* $A^+_{({\rm OT};j)}$ and $A^+_{({\rm LIB};j)}$ are computed according to the sine and cosine coefficients given in Tables 8.2a and 5.1a of the IERS 2010 conventions (Petit & Luzum 2010).

The pole coordinates (x, y) can be represented by

$$x = x_{C04} + \Delta x; \quad y = y_{C04} + \Delta y, \qquad (15)$$

where (x_{C04}, y_{C04}) are the pole coordinates from *C*04 series (Bizouard *et al.* 2018) and $(\Delta x, \Delta y)$ are the variation of pole coordinate in the subdiurnal band. The global adjustment of A_j^+ requires the

Table 1. The main terms of the ocean's angular momentum and their corresponding oceanic Love number ($\tilde{k}_o$). The angular momentum is generated by tesseral diurnal gravitational tides based on the FES 2014 model. The amplitudes H_1, H_2, h_1 and h_2 are in the unit of 10^{25} kg m^2 s^{-1}.

	Period (d)	H_1	Φ_1 (°)	H_2	Φ_2 (°)	h_1	ϕ_1 (°)	h_2	ϕ_2 (°)	$\tilde{k}_o$
$Q1$	1.1195148	0.110	340.1	0.269	214.9	0.063	301.6	0.069	209.7	$0.005 + i\,0.019$
$O1$	1.0758059	0.449	327.4	1.192	222.8	0.313	301.9	0.449	201.0	$0.008 + i\,0.016$
$P1$	1.0027454	0.159	309.3	0.445	226.7	0.174	293.2	0.255	193.8	$0.008 + i\,0.012$
$K1$	0.9972695	0.481	307.3	1.325	227.2	0.545	293.7	0.805	193.3	$0.008 + i\,0.012$
$J1$	0.9624365	0.029	301.9	0.076	227.0	0.018	297.1	0.044	179.6	$0.007 + i\,0.016$

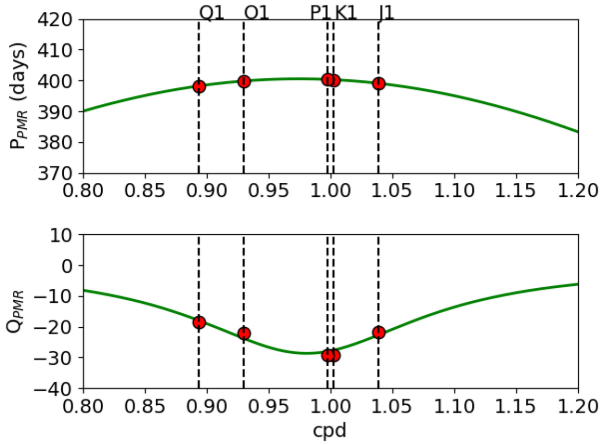

Figure 1. The period and the equivalent quality factor of PMR in diurnal prograde band calculated from the FES 2014 ocean model. The red points correspond to the five discrete tidal lines for which PMR parameters are deduced, as reported in Table 1.

partial derivatives of the time delay with respect to A_j^+, namely

$$\frac{\partial \tau}{\partial A_j^+} = c^{-1} \cdot \underline{k} \cdot Q(X, Y) \cdot R(-\theta) \cdot \frac{\partial W(x, y)}{\partial A_j^+} \cdot \underline{b}, \tag{16}$$

where c is the speed of light, $\underline{k}$ is the unit vector pointing in the source direction expressed in the ICRF, $\underline{b}$ is the baseline unit vector expressed in the ITRF, θ is the Earth rotation angle between the celestial and terrestrial intermediate origin, and X and Y are the full Cartesian coordinates of the celestial pole in the International Celestial Reference System. We implement those partial derivatives in the geodetic analysis software Calc/Solve (Ma *et al.* 1986) to find the corrections for 72 terms contained in the IERS model.

The data, taken from the IVS data centre, are made up of 5452 VLBI sessions from 1990 to 2020. We estimated station coordinate differences with respect to ITRF2014 (Altamimi *et al.* 2016) as global parameters with no-net rotation and no-net translation conditions applied to the positions and velocities of a group of 38 stations. Apriori station positions were corrected from tridimensional displacements due to oceanic and atmospheric tidal loading using FES2004 (Lyard *et al.* 2006) and the output from the inverted-barometer version of the Atmospheric Pressure Loading Service (APLO; Petrov & Boy 2004) as well as antenna thermal deformations (Nothnagel 2009). A no-net rotation condition was applied to the 303 ICRF3 defining sources (Charlot *et al.* 2020). Apriori dry zenith delays were estimated from local pressure values and then mapped to the elevation using the Vienna Mapping Function (Böhm *et al.* 2006). The modelling of intraday variations of the troposphere wet delay, clocks and troposphere gradients was realized through continuous piecewise linear functions whose coefficients are estimated every 10 min, 30 min, and 6 hr, respectively. Apriori Earth orientation parameters were taken from the *C*04 (Bizouard *et al.* 2018) and the IAU 2000A/IAU 2006 nutation and precession models (Mathews *et al.* 2002; Capitaine *et al.* 2003).

The inversion returned a post-fit rms of 25.83 picoseconds and a χ^2 per degree of freedom equal to 1.06. The results of our estimation for 19 major diurnal tidal components are displayed in Table 2 and compared with independent studies of the last decade, including the IERS model. We found no significant correlation between the estimated tidal terms. The published estimates of the tidally induced polar motion are commonly given as sine and cosine coefficients of the pole coordinates at a given frequency:

$$\begin{aligned} x &= C_x \cos\theta(t) + S_x \sin\theta(t), \\ y &= C_y \cos\theta(t) + C_y \sin\theta(t). \end{aligned} \tag{17}$$

The corresponding prograde polar motion $A^+ = \alpha e^{i\Theta}$ is given through

$$\begin{aligned} \alpha &= \frac{1}{2}\sqrt{(C_x - S_y)^2 + (S_x + C_y)^2}, \\ \Theta &= \arctan\left(-\frac{(S_x + C_y)}{(C_x - S_y)}\right). \end{aligned} \tag{18}$$

Our estimates are consistent with Artz *et al.* (2011) within 3σ level for all main diurnal terms ($Q1$, $O1$, $P1$, $K1$ and $J1$). However, we have discrepancies for the other terms. Such disagreements also occur with the estimates of Böhm *et al.* (2012). The different time intervals between ours (1990–2020), Artz *et al.* (2011) (1980–2010) and Böhm *et al.* (2012) (1984–2010.5) as well as the different VLBI analysis strategies are the sources of these discrepancies. The difference with Sibois *et al.* (2017) results may be caused by systematic errors from GNSS or VLBI. On the other hand, our least-squares formal errors may be underestimated. As mentioned by Herring *et al.* (2002), these values can be underestimated by a factor between 1.5 and 2. Meanwhile, for some terms each empirical model differs significantly from the IERS values. These disagreements have provoked the need to both refine the theoretical modelling or to improve the quality of the observation itself.

5 POLAR MOTION RESONANCE ESTIMATION

In the frequency domain, the dynamical relation (8) reads

$$p(\sigma) = -\frac{\tilde{\sigma}_{\mathrm{PMR}}}{\sigma - \tilde{\sigma}_{\mathrm{PMR}}} \chi^{\mathrm{eff}}(\sigma). \tag{19}$$

The effective angular momentum function $\chi^{\mathrm{eff}}(\sigma)$ takes the form

$$\chi^{\mathrm{eff}}(\sigma) = \frac{1}{1 - \frac{\tilde{k}_2 + \tilde{k}_o(\sigma)}{k_s}} \left[\left(1 + k_2^{'}\right) \chi_{\mathrm{ma}}(\sigma) + \chi_{\mathrm{mo}}(\sigma)\right], \tag{20}$$

Table 2. Diurnal prograde terms estimated from VLBI observation over the period 1990–2020, the terms derived from IERS ocean tides model and the terms estimated from Sibois *et al.* (2017, SD17), Böhm *et al.* (2012, B12) and Artz *et al.* (2011, AB11). The diurnal terms that are used for the resonance estimation are highlighted in bold. Here the unit of components are μas and the formal error corresponds to their 3σ.

		This work				IERS		SD17		B12		AB11	
Tide	Period (d)	A^+_{IP}	±	A^+_{OP}	±	A^+_{IP}	A^+_{OP}	A^+_{IP}	A^+_{OP}	A^+_{IP}	A^+_{OP}	A^+_{IP}	A^+_{OP}
$Q1$	1.166926	6.47	2.81	−4.64	2.82	3.4	−0.3	3.6	1.9	4.0	0.2	10.9	−0.1
$\sigma 1$	1.160349	3.44	2.8	−2.84	2.79	4.15	−0.5	4.9	−0.9	5.4	−1.4	6.7	−5.5
Q1	**1.119515**	**30.43**	**2.92**	**−8.1**	**2.91**	**27.6**	**−3.9**	**31.7**	**−8.4**	**24.8**	**−7.2**	**28.1**	**−8.5**
RO1	1.113461	3.4	2.72	−1.73	2.72	5.3	−0.9	5.8	−2.6	1.5	−0.2	6.2	−2.1
O1	**1.075806**	**138.29**	**2.81**	**−46.8**	**2.81**	**139.4**	**−37.4**	**133.8**	**−54.9**	**125.0**	**−59.2**	**138.9**	**−45.5**
TO1	1.069505	1.13	2.67	−0.49	2.68	1.7	−0.7	0.8	−2.0	0.5	0.6	3.3	−2.2
$M1$	1.034719	8.67	2.57	−3.85	2.56	10.1	−3.7	8.9	−4.4	6.9	−3.2	5.6	−6.5
$\chi 1$	1.029545	0.65	2.44	0.08	2.43	1.8	−0.9	1.9	−0.3	3.2	−0.2	1.8	−0.9
$\pi 1$	1.005506	−0.5	2.39	−5.3	2.39	3.0	−1.5	5.2	−4.0	2.2	−1.4	5.1	−4.3
P1	**1.002745**	**51.07**	**2.57**	**−26.63**	**2.58**	**53.9**	**−21.3**	**48.3**	**−27.4**	**44.2**	**−27.6**	**52.4**	**−26.3**
$S1$	1.000000	0.29	2.5	−8.51	2.43	1.2	−0.6	5.3	−0.9	10.6	11.2	8.8	10.4
K1	**0.997270**	**165.1**	**2.7**	**−88.62**	**2.68**	**159.9**	**−63.2**	**148.3**	**−99.6**	**158.3**	**−101.6**	**165.5**	**−90.5**
$\phi 1$	0.994554	1.56	2.45	−2.17	2.44	1.2	−0.6	1.6	3.5	2.1	−0.1	2.3	−3.0
$\varphi 1$	0.991853	−0.59	2.35	−4.42	2.35	2.1	−1.1	0.9	−0.1	1.9	5.2	3.5	1.2
TT1	0.966956	2.98	2.25	0.35	2.25	1.4	−0.7	1.9	−0.1	1.2	−1.1	1.4	−0.7
J1	**0.962437**	**10.15**	**2.34**	**−2.54**	**2.34**	**7.7**	**−2.7**	**6.7**	**−6.9**	**9.2**	**−5.7**	**8.2**	**−1.4**
So1	0.934174	0.53	2.16	1.18	2.18	1.1	−0.4	0.2	1.0	1.3	−2.2	1.2	4.4
Oo1	0.929420	4.85	2.24	−5.19	2.24	3.4	−1.1	4.1	−4.8	1.9	−8.9	4.5	−7.9
$\nu 1$	0.899093	1.1	2.2	2.15	2.2	0.6	0.0	0.1	−1.9	3.7	−0.8	4.3	1.7

where k'_2 is loading Love number, χ_{ma} and χ_{mo} are the mass and motion terms of the effective angular momentum function respectively. By considering eqs (9) and (20), eq. (19) is rewritten as follows:

$$p(\sigma) = \frac{eA\Omega}{A_m}\left[-\frac{1}{\sigma - \tilde{\sigma}_{PMR}}\left((1+k'_2)\chi_{ma}(\sigma) + \chi_{mo}(\sigma)\right)\right]. \quad (21)$$

Considering the five main tidal frequencies ($Q1$, $O1$, $P1$, $K1$ and $J1$), the PMR parameters are overdetermined by a set of five complex eqs (21) relating corresponding terms of the polar motion and of the tidal angular momentum function. However, this system is ill-conditioned for a least-squares inversion, since in eq. (21) the influence of $\tilde{\sigma}_{PMR} \sim \Omega/400$ is totally mitigated by $\sigma \sim \Omega$. So, this system will be formed with a more appropriate relation. By defining $\chi_o(\sigma) = (1+k'_2)\chi_{ma}(\sigma) + \chi_{mo}(\sigma)$, eq. (21) becomes

$$p(\sigma) = \frac{eA\Omega}{A_m}\left(-\frac{\chi_o(\sigma)}{\sigma - \tilde{\sigma}_{PMR}}\right). \quad (22)$$

As $\chi_o = \tilde{k}_o/k_s\,\tilde{\Phi}$, we obtain

$$p(\sigma) = \frac{eA\Omega}{A_m}\left(-\frac{\tilde{k}_o}{k_s}\frac{\tilde{\Phi}(\sigma)}{\sigma - \tilde{\sigma}_{PMR}}\right). \quad (23)$$

By considering eq. (9), the ocean love number is rewritten in terms of $\tilde{\sigma}_{PMR}$:

$$\tilde{k}_o = -\tilde{k}_2 + k_s\left(1 - \frac{A_m}{eA\Omega}\tilde{\sigma}_{PMR}\right). \quad (24)$$

Substituting $\tilde{k}_o$ in eq. (23) with eq. (24) leads to

$$p(\sigma) = \left[-\frac{1}{\sigma - \tilde{\sigma}_{PMR}}\left(\frac{eA\Omega}{A_m}\left(1 - \frac{\tilde{k}_2}{k_s}\right) - \tilde{\sigma}_{PMR}\right)\right]\tilde{\Phi}(\sigma). \quad (25)$$

The PMR parameters are estimated from eq. (25) by fitting the five dominant prograde diurnal terms in Table 2, as determined from VLBI or GNSS observation, to the corresponding tidal potential $\tilde{\Phi}(\sigma)$. As the prograde diurnal terms are assumed to reflect only the influence of the ocean tides, the 'libration' effect, caused by the coupling between lunisolar diurnal tides and triaxiality, has to be eliminated before performing the inversion. We adopt the libration model recommended in IERS conventions (Table 5.1a of IERS Conventions 2010).

Table 3. Estimates of the PMR parameters (period and equivalent quality factor) in the prograde diurnal band. The confidence interval corresponds to their 1σ. Note that these parameters are relative to the terrestrial reference system.

	Period (d)	Q_{PMR}
Sibois *et al.* (2017)	**401.24** (400.32, 402.17)	**−23** (−25, −22)
Artz *et al.* (2011)	**400.81** (400.16, 401.45)	**−22** (−24, −21)
Böhm *et al.* (2012)	**401.04** (400.39, 401.69)	**−24** (−25, −23)
This study	**400.84** (400.13, 401.55)	**−22** (−24, −21)

The PMR parameters are estimated for each of the four sets of *observed* prograde diurnal components (limited to the five dominant terms reported in boldface in Table 2). In the estimation, the error of each prograde diurnal term is chosen as the maximum difference between the four considered values. Results are given in Table 3. Accounting for error bars, all estimated values can be represented by $P_{PMR} = 401 \pm 1$ d and to an equivalent quality factor Q_{PMR} in the interval $(-24, -21)$. In regard to our study, the closest estimates of the main prograde diurnal terms are those of Artz *et al.* (2011), and it is not surprising to found this closeness in the corresponding PMR parameters. The estimates match strikingly the theoretical values that are more loosely determined: $P_{PMR} = [398, 400]$ days and $Q_{PMR} = [-29, -18]$ according to Fig. 1. Considering more diurnal terms, we found that the estimate parameters are not affected significantly.

We also test the sensitivity of the PMR parameters to each prograde diurnal term by reducing the observation matrix of the fit to four prograde terms. The results, reported in Table 4, show that the estimate of the period is mostly sensitive to the removal of the term $O1$. By neglecting this term, the period decreases by about 1 d, becoming 400 d. Meanwhile, the equivalent quality factor is slightly changed to $(-23, -20)$ if we ignore $P1$ term in the estimation.

Table 4. The PMR parameters (period and equivalent quality factor) estimated from $Q1$, $O1$, $P1$, $K1$ and $J1$ terms by excluding one of them. Note that these parameters are relative to the terrestrial reference system.

Ignored term	Period (d)	Q_{PMR}
$Q1$	**400.05** (399.24, 400.86)	**−22** (−24, −21)
$O1$	**399.91** (399.04, 400.78)	**−22** (−24, −21)
$P1$	**400.43** (399.45, 401.42)	**−21** (−23, −20)
$K1$	**400.72** (399.75, 401.68)	**−22** (−24, −21)
$J1$	**400.86** (400.05, 401.68)	**−22** (−24, −21)
None	**400.84** (400.13, 401.55)	**−22** (−24, −21)

6 CONCLUSIONS

This study aimed at determining the PMR parameters in the prograde diurnal band [0.8, 1.2] cpd. This is a logical extension of Bizouard *et al.* (2020) focused on the retrograde diurnal band of the polar motion, namely the nutation band of the Celestial Intermediate Pole.

First, a theoretical prediction was built according to the body Love number of an anelastic Earth, recommended in IERS conventions 2010, and the updated oceanic tidal model FES 2014: it led to the conclusion that the PMR parameters slightly depend on frequency throughout the prograde diurnal band, with a period ranging from 390 to 400 d, and an equivalent quality factor lying in the interval [−30, −8]. This period is located between the Chandler wobble period of 433 d and the value obtained in the retrograde diurnal band (380 d). The negative equivalent quality factor reflects the dynamical response to the diurnal components of lunisolar tide potential, which contain a strong out-of-phase part.

Second, the PMR parameters are determined by confronting the observed prograde diurnal terms, directly adjusted from VLBI delay or GNSS observations, to the lunisolar diurnal tesseral potential, which is the dominant cause of those terms. We complete three recent published sets with our own VLBI estimates obtained over the period 1990–2020 through a direct approach.

We conclude that, in the band [0.89, 1.04] cpd, the PMR has a period $P_{\mathrm{PMR}} = 400.8 \pm 0.7$ d and an equivalent quality factor Q_{PMR} in the interval (−24, −21). This fits the corresponding theoretical prediction of the period (399.5 ± 0.8 d) and of the equivalent quality factor ($-29 \leq Q_{\mathrm{PMR}} \leq -18$). Furthermore, we have tested the sensitivity of our results with respect to each prograde term and show that the estimates are mostly sensitive to $O1$ term for the period and $P1$ for the equivalent quality factor.

The increasing accuracy of Earth rotation changes and modelling of their excitation allow to determine the frequency-dependent Earth rheology from diurnal timescale to some decades. Until the 2000s, this approach was limited to length-of-day changes caused by the zonal tides; now it pertains also to the polar motion components excited by diurnal tesseral tides. In this case, the global rheological parameters given by the Love numbers are manifested by the values of the PMR complex frequency, which is itself frequency-dependent. The accurate knowledge of this frequency dependence not only constraints the Earth rheology, but also leads to a better model the PMR changes from reconstructed forcing. It remains to investigate semi-diurnal and rapid bands (between 2 and 20 d), where the dynamical effects of the oceans are also determining.

ACKNOWLEDGEMENTS

We are grateful to Dr Florent Lyard for his participation in the computation of the tidal components and the ocean angular momentum function from the outputs of the FES 2014 model. We acknowledge the two anonymous reviewers for their useful comments that helped us to improve the paper.

DATA AVAILABILITY

The data underlying this article will be shared on reasonable request to the corresponding author.

REFERENCES

Altamimi, Z., Rebischung, P., Métivier, L. & Collilieux, X., 2016. ITRF2014: a new release of the International Terrestrial Reference Frame modeling nonlinear station motions, *J. geophys. Res.,* **121**(8), 6109–6131.

Artz, T., Tesmer, S. & Nothnagel, A., 2011. Assessment of periodic sub-diurnal Earth rotation variations at tidal frequencies through transformation of VLBI normal equation systems, *J. Geod.,* **85**(9), 565–584.

Bizouard, C., 2020. *Geophysical Modelling of the Polar Motion,* De Gruyter.

Bizouard, C., Lambert, S., Gattano, C., Becker, O. & Richard, J.-Y., 2018. The IERS EOP 14C04 solution for Earth orientation parameters consistent with ITRF 2014, *J. Geod.,* **93,** 621–633.

Bizouard, C., Nurul Huda, I., Ziegler, Y. & Lambert, S., 2020. Frequency dependence of the polar motion resonance, *Geophys. J. Int.,* **220**(2), 753–758.

Böhm, J., Werl, B. & Schuh, H., 2006. Troposphere mapping functions for GPS and very long baseline interferometry from European Centre for Medium-Range Weather Forecasts operational analysis data, *J. geophys. Res.,* **111**(B2), doi:10.1029/2005JB003629.

Böhm, S., Brzeziński, A. & Schuh, H., 2012. Complex demodulation in VLBI estimation of high frequency Earth rotation components, *J. Geodyn.,* **62,** 56–68.

Capitaine, N., Wallace, P.T. & Chapront, J., 2003. Expressions for IAU 2000 precession quantities, *Astron. Astrophys.,* **412**(2), 567–586.

Carrere, L., Lyard, F., Cancet, M. & Guillot, A., 2015. FES 2014, a new tidal model on the global ocean with enhanced accuracy in shallow seas and in the arctic region, in *EGU General Assembly,* EGU, Vienna, Austria, p. 5481.

Charlot, P., *et al.*, 2020. The third realization of the International Celestial Reference Frame by very long baseline interferometry, *Astron. Astrophys.,* **644,** A159, doi:10.1051/0004-6361/202038368.

Dehant, V. & Mathews, P., 2015. *Precession, Nutation and Wobble of the Earth,* p. 554, Cambridge Univ. Press.

Furuya, M. & Chao, B.F., 1996. Estimation of period and Q of the Chandler wobble, *Geophys. J.,* **127**(3), 693–702.

Gipson, J.M., 1996. Very long baseline interferometry determination of neglected tidal terms in high-frequency Earth orientation variation, *J. geophys. Res.,* **101**(B12), 28 051–28 064.

Herring, T.A. & Dong, D., 1994. Measurement of diurnal and semidiurnal rotational variations and tidal parameters of Earth, *J. geophys. Res.,* **99**(B9), 18 051–18 071.

Herring, T.A., Mathews, P.M. & Buffett, B.A., 2002. Modeling of nutation-precession: very long baseline interferometry results, *J. geophys. Res.,* **107**(B4), ETG 4–1-ETG 4-12.

Kuehne, J., Wilson, C.R. & Johnson, S., 1996. Estimates of the Chandler wobble frequency and Q, *J. geophys. Res.,* **101,** 13 573–13 580.

Lyard, F., Lefevre, F., Letellier, T. & Francis, O., 2006. Modelling the global ocean tides: modern insights from FES2004, *Ocean Dyn.,* **56**(5–6), 394–415.

Ma, C., *et al.*, 1986. Radio-source positions from VLBI, *Astron. J.,* **92,** 1020–1029.

Mathews, P.M., Herring, T.A. & Buffett, B.A., 2002. Modeling of nutation and precession: new nutation series for nonrigid Earth and insights into the Earth's interior, *J. geophys. Res.,* **107**(B4), ETG–3-ETG-26.

Nastula, J. & Gross, R., 2015. Chandler wobble parameters from SLR and GRACE, *J. geophys. Res.,* **120,** 4474–4483.

Nothnagel, A., 2009. Conventions on thermal expansion modelling of radio telescopes for geodetic and astrometric VLBI, *J. Geod.,* **83**(8), 787–792.

Nurul Huda, I., Lambert, S., Bizouard, C. & Ziegler, Y., 2020. Nutation terms adjustment to VLBI and implication for the Earth rotation resonance parameters, *Geophys. J. Int.,* **220**(2), 759–767.

Petit, G. & Luzum, B., 2010. IERS Conventions 2010, IERS Technical Note 36, Frankfurt am Main: Verlag des Bundesamts für Kartographie und Geodäsie, 179 pp.

Petrov, L. & Boy, J.-P., 2004. Study of the atmospheric pressure loading signal in very long baseline interferometry observations, *J. geophys. Res.,* **109**(B3), doi:10.1029/2003JB002500.

Ray, R.D., Steinberg, D.J., Chao, B.F. & Cartwright, D.E., 1994. Diurnal and semidiurnal variations in the earth's rotation rate induced by oceanic tides, *Science,* **264**(5160), 830–832.

Rosat, S., Lambert, S., Gattano, C. & Calvo, M., 2016. Earth's core and inner-core resonances from analysis of VLBI nutation and superconducting gravimeter data, *Geophys. Suppl. Mon. Not. R. Astron. Soc.,* **208**(1), 211–220.

Sibois, A.E., Desai, S.D., Bertiger, W. & Haines, B.J., 2017. Analysis of decade-long time series of GPS-based polar motion estimates at 15-min temporal resolution, *J. Geod.,* **91**(8), 965–983.

Sovers, O., Jacobs, C. & Gross, R., 1993. Measuring rapid ocean tidal Earth orientation variations with very long baseline interferometry, *J. geophys. Res.,* **98**(B11), 19 959–19 971.

Vondrák, J., Ron, C. & Chapanov, Y., 2017. New determination of period and quality factor of chandler wobble, considering geophysical excitations, *Adv. Space Res.,* **59**(5), 1395–1407.

Watkins, M.M. & Eanes, R.J., 1994. Diurnal and semidiurnal variations in Earth orientation determined from LAGEOS laser ranging, *J. geophys. Res.,* **99**(B9), 18 073–18 079.

Ziegler, Y., Lambert, S.B., Nurul Huda, I., Bizouard, C. & Rosat, S., 2020. Contribution of a joint Bayesian inversion of VLBI and gravimetric data to the estimation of the free inner core nutation and free core nutation resonance parameters, *J. geophys. Int.,* **222**(2), 845–860.